

Article

Cutaneous Regeneration Mechanism of β -Sheet Silk Fibroin in a Rat Burn Wound Healing Model

Kai-Chieh Chou ^{1,†}, Chun-Ting Chen ^{2,3,†}, Juin-Hong Cherng ^{1,4,5} , Ming-Chia Li ⁶, Chia-Cheng Wen ⁷, Sheng-I Hu ⁷ and Yi-Wen Wang ^{1,5,*} 

- ¹ Graduate Institute of Life Sciences, National Defense Medical Center, Taipei 114, Taiwan; jeffrey8464@gapps.ndmctsgh.edu.tw (K.-C.C.); i72bbb@gmail.com (J.-H.C.)
 - ² Division of Gastroenterology and Hepatology, Department of Internal Medicine, Tri-Service General Hospital Penghu Branch, National Defense Medical Center, Taipei 114, Taiwan; gp0921543gp@yahoo.com.tw
 - ³ Division of Gastroenterology and Hepatology, Department of Internal Medicine, Tri-Service General Hospital, National Defense Medical Center, Taipei 114, Taiwan
 - ⁴ Laboratory of Adult Stem Cell and Tissue Regeneration, National Defense Medical Center, Taipei 114, Taiwan
 - ⁵ Department and Graduate Institute of Biology and Anatomy, National Defense Medical Center, Taipei 114, Taiwan
 - ⁶ Department of Biological Science and Technology, Center For Intelligent Drug Systems and Smart Bio-Devices (IDS2B), National Yang Ming Chiao Tung University, Hsinchu 300, Taiwan; mingchiali@g2.nctu.edu.tw
 - ⁷ Division of Colon and Rectal Surgery, Department of Surgery, Tri-Service General Hospital, National Defense Medical Center, Taipei 114, Taiwan; wjason@mail2000.com.tw (C.-C.W.); roger720922@msn.com (S.-I.H.)
- * Correspondence: christmas1035@mail.ndmctsgh.edu.tw; Tel.: +886-2-8792-3100 (ext. 18749); Fax: +886-2-87923767
- † These authors contributed equally to this work.



Citation: Chou, K.-C.; Chen, C.-T.; Cherng, J.-H.; Li, M.-C.; Wen, C.-C.; Hu, S.-I.; Wang, Y.-W. Cutaneous Regeneration Mechanism of β -Sheet Silk Fibroin in a Rat Burn Wound Healing Model. *Polymers* **2021**, *13*, 3537. <https://doi.org/10.3390/polym13203537>

Academic Editor: Shiao-Wei Kuo

Received: 14 September 2021

Accepted: 11 October 2021

Published: 14 October 2021

Publisher's Note: MDPI stays neutral with regard to jurisdictional claims in published maps and institutional affiliations.



Copyright: © 2021 by the authors. Licensee MDPI, Basel, Switzerland. This article is an open access article distributed under the terms and conditions of the Creative Commons Attribution (CC BY) license (<https://creativecommons.org/licenses/by/4.0/>).

Abstract: Therapeutic dressings to enhance burn wound repair and regeneration are required. Silk fibroin (SF), a natural protein, induces cell migration and serves as a biomaterial in various dressings. SF dressings usually contain α -helices and β -sheets. The former has been confirmed to improve cell proliferation and migration, but the wound healing effect and related mechanisms of β -sheet SF remain unclear. We investigated the effects of β -sheet SF in vivo and in vitro. Alcohol-treated α -helix SF transformed into the β -sheet form, which promoted granulation formation and re-epithelialization when applied as lyophilized SF dressing (LSFD) in a rat burn model. Our in vitro results showed that β -sheet SF increased human dermal fibroblast (HDF) migration and promoted the expression of extracellular matrix (ECM) proteins (fibronectin and type III collagen), matrix metalloproteinase-12, and the cell adhesion molecule, integrin β 1, in rat granulation tissue and HDFs. This confirms the role of crosstalk between integrin β 1 and ECM proteins in cell migration. In summary, we demonstrated that β -sheet SF facilitates tissue regeneration by modulating cell adhesion molecules in dermal fibroblasts. LSFD could find clinical application for burn wound regeneration. Moreover, β -sheet SF could be combined with anti-inflammatory materials, growth factors, or antibiotics to develop novel dressings.

Keywords: burn injury; wound healing; β -sheet silk fibroin; cell migration; integrin; extracellular matrix protein; *Bombyx mori*

1. Introductions

Burn injuries cause severe damage to the epidermis, dermis, and underlying tissue, often resulting in physical and mental illnesses [1]. Ideally, burn wound dressings should be infection-resistant, retain moisture, and facilitate tissue regeneration [2]. Biomaterials applied in wound dressings have been reported to induce cell migration, re-epithelialization, and granulation tissue formation during the proliferation phase of cutaneous wound healing [3–5].

Silk, derived from *Bombyx mori* cocoons, is a well-known and favored natural proteinaceous fiber with a long history of utilization in textiles. One of its main components is silk fibroin (SF). The structure of SF is characterized by macromolecules with three amino acids in repeating sequences (Gly–Ser–Gly–Ala–Gly–Ala) [6,7]. SF is biodegradable and biocompatible, and has been applied in surgical sutures, skincare products [8,9], and tissue engineering in the skin [10], cartilage [11], and corneal repair [12]. Additionally, SF has been developed into several forms of dressings, including sponges, films, scaffolds, electrospun nanofibers, and hydrogels [13,14]. Silk fibroin exists in alpha-helix and beta-sheet form, both of which are highly biocompatible and can also promote tissue regeneration [13,15]. However, it is difficult for amorphous silk fibroin (α -helix or random coil) to form stable scaffolds [16,17]. β -sheet silk fibroin provides good mechanical properties and structure for cell attachment; moreover, it shows a nontoxic influence on fibroblasts and stem cells [18,19], facilitation in collagen deposition during bone regeneration [19], and promotion for angiogenesis during wound healing [20]. For building a structurally stable scaffold and a biomaterial for wound dressing, the β -sheet form SF was prioritized [21,22]. It has been reported that lyophilized SF scaffolds possess biocompatible properties and pores optimized for cell growth [19,23]. Alcohol treatment of lyophilized SF induces the transition of the α -helices to β -sheets to form a stable wound dressing [24]. We aimed to evaluate whether this lyophilized SF dressing (LSFD) could promote burn wound healing.

During the proliferation phase, extracellular matrix (ECM) deposition is essential for cell adhesion, which promotes cell migration during wound re-epithelialization and granulation. Natural SF has a hydrophilic soluble α -helix form and a self-crystalline insoluble β -sheet form [6,25]. It has been reported that α -helix SF induces the gene expression of the mechanistic target of rapamycin (mTOR) axis and cell adhesion molecules, and elevates ECM protein expression via the nuclear factor kappa B (NF- κ B) signaling pathway in human dermal fibroblasts (HDFs) [26]. However, LSFD is mainly composed of β -sheet SF, and the effect and related mechanism of β -sheet SF on ECM expression and cell migration during wound healing remain unclear.

Integrins, which are cell adhesion molecules, are cell surface receptors and are composed of α - and β -subunits that specifically contact ECM proteins [27]. This facilitates multiple cellular activities, including cell migration and cytoskeleton modulation [27,28]. In vitro studies have shown that SF increases integrin expression in human umbilical vein endothelial cells [26,29,30]. These in vitro data showed that SF treatment potentially promotes cell motility by increasing integrin expression and ultimately results in wound regeneration. However, this inference has not been confirmed in skin cells and animal wound model. Therefore, we determined integrin expression after β -sheet SF treatment in HDFs and burn wounds in rats.

In this study, we aimed to investigate the effect and underlying mechanism of β -sheet SF in HDFs and keratinocytes, and evaluate the effect of lyophilized SF dressing (LSFD) in a rat burn wound healing model by analyzing granulation tissue formation and wound re-epithelialization. These results suggest that LSFD could be applied clinically to improve burn wound regeneration. Moreover, the β -sheet SF structure could lend stability to combinations with other anti-inflammatory materials, growth factors, or antibiotic reagents, to develop novel dressings with ideal characteristics to promote burn wound regeneration.

2. Materials and Methods

2.1. SF Solution Extraction and Characterization

The extraction of the SF aqueous solution complied with previous research [26,31,32]. Silk cocoons of *B. mori* were purchased from Danee Company (New Taipei City, Taiwan). Briefly, to remove the silk sericin coating, the cocoons were cut into pieces and degummed for 30 min with a 0.02 M Na₂CO₃ solution at 100 °C. After washing with distilled water and drying overnight in an oven at 37 °C, degummed fibers were dissolved in a 9.3 M LiBr solution at 60 °C for 6 h. Until the degummed fibers were solubilized, this silk solution was dialyzed in distilled water at room temperature for three days using dialysis membranes

(Cellu-Sep; nominal molecular weight cutoff: 12,000–14,000; Interchim, Montluçon, France). The dialyzed silk solution was centrifuged at 500 rpm for 20 min. The final concentration of SF solution was approximately 5–6% (*w/v*), determined by weighing the residual solid after oven-drying at 37 °C. The SF aqueous solution was stored at 4 °C until required for further use. The SF aqueous solution was coated onto a quartz plate. After evaporation, a 75% ethanol solution was added. Circular dichroism (CD) spectra were measured and recorded using a J-1700 CD spectrophotometer (Jasco Inc., Easton, MD, USA).

2.2. LSFDF Preparation

The preparation of LSFDF by lyophilization was performed using a method we had published before [19]. After freeze-drying based on temperature modulation, LSFDF was obtained via β -sheet crystallization using a 75% ethanol solution treatment. The ethanol solution was removed by complete evaporation in a hood. Then, the LSFDFs were stored at room temperature until required. The pore size is approximately 170 μm in diameter, and 75% of pores are interconnected [19].

2.3. Rat Burn Model

Seven Sprague–Dawley rats (150–200 g; 7 weeks old) were purchased from Bio-LASCO Co., Ltd. (Taipei City, Taiwan). The burning procedure was performed according to Wang et al. [33], and all animal experiments were approved by and conducted in accordance with the National Defense Medical Center Institutional Animal Care and Use Committee (IACUC-20-016). A total of 12 female rats were used in this study: five rats for the condition test and seven for the repeat experiment and data analysis. Before the burn wound was created using a 2-cm diameter brass block at 100 °C for 10 s, the rats were shaved dorsally and received anesthesia via intramuscular injection of Zoletil 50 (20 mg/kg; Virbac, Carros, France) in the calf area. Two parallel burn wounds were created on the back of each rat; the distance between the two wound edges was approximately 3 cm. The heated brass block caused second-degree burn wounds [34]; the wounds were covered with gauze and Tegaderm transparent film dressing (3M Health Care, St. Paul, MN, USA) to prevent scratching. All the rats were housed individually in cages under aseptic conditions after surgery.

After wounding on day 0, debridement was performed the next day (day 1). The two burn wounds on each rat were covered with gauze (control group) or LSFDF (LSFDF group), respectively. The animals were kept warm with an electrically heated blanket during the surgery, and received daily intramuscular injections of ketoprofen (2.5 mg/kg; Astar, Hsinchu, Taiwan) for analgesia and cefazolin (25 mg/kg; China Chemical & Pharmaceutical, Taipei City, Taiwan) to prevent infection after surgery. Each wound was disinfected daily with iodine solution and cleaned with sterile normal saline, cotton swabs, and gauze.

2.4. Wound Closure Analysis

The burn wounds were recorded with a digital camera on days 0, 1, 3, 7, and 10, and the wound area was measured using ImageJ software (19 January 2021 accessed, <https://imagej.nih.gov/ij/>; NIH, Bethesda, MD, USA). The gauze and LSFDF were replaced after the wound was recorded. The wound closure rate was computed by two blinded evaluators and expressed as the percentage of the initial wound size.

2.5. Histological Analysis

All rats were euthanized on day 10. The wound area and surrounding normal tissue were harvested and cut into halves; one piece was immediately fixed in 4% paraformaldehyde solution for section staining, and the other was frozen in liquid nitrogen for Western blot analysis. After fixation, the tissues were embedded in paraffin. The sections (5 μm) were stained with hematoxylin and eosin (H&E) (Merck Millipore, Darmstadt, Germany) and Masson's trichrome stain kit (ScyTek Laboratories, Logan, UT, USA), following the

manufacturer's protocol. The stained sections were viewed and photographed using an Axio Scan Z1 slide scanner (ZEISS, Oberkochen, Germany).

2.6. Immunohistochemistry (IHC) Staining

The 5 μm tissue sections were dewaxed with xylene (Ferak Berlin, Germany) and rehydrated. Each section was blocked with 10% normal goat serum in phosphate-buffered saline (PBS) for 1 h and then incubated with the primary antibody in blocking solution at room temperature for 1 h. The following primary antibodies were used for staining: mouse anti-vitronectin, mouse anti-fibronectin (FN), mouse anti-integrin $\alpha 1$, mouse anti-integrin $\alpha 2$, mouse anti-integrin $\alpha 5$, mouse anti-integrin αv , mouse anti-integrin $\beta 1$, mouse anti-integrin $\beta 3$, (sc-74484, sc-8422, sc-271034, sc-74466, sc-376199, sc-376156, sc-374429, and sc-365679, respectively, 1:1000, Santa Cruz Biotechnology, Inc., Dallas, TX, USA), mouse anti-collagen I, rabbit anti-collagen III, rabbit anti-matrix metalloproteinase-1 (MMP-1), rabbit anti-MMP-12, rabbit anti-MMP-13, mouse anti- α -smooth muscle actin (SMA) (GTX26308, GTX102997, GTX00674, GTX100704, GTX100665, GTX629702, respectively; 1:1000; GeneTex, Irvine, CA, USA). After removing the immersing solution, all sections were washed three times for 5 min with PBS and then incubated with the second antibody containing biotin. After washing, sections were soaked using an ABC kit (Vector Laboratories, Inc., Burlingame, CA, USA) for 1 h and visualized using 3,3'-diaminobenzidine solution containing 3% hydrogen peroxide. All the tissue sections were then counterstained with hematoxylin and photographed using an Axio Scan Z1 slide scanner (ZEISS).

2.7. Immunofluorescence Staining

The frozen tissue sections (20 μm) were washed with PBS and blocked with 0.1% goat serum in PBS for 30 min. The keratin-14 (K14) antibody diluted in blocking solution was used at a 1:1000 dilution for 1 h. After washing with PBS, the tissue samples were incubated with goat anti-mouse IgG secondary antibody (Alexa Fluor 488, 1:1000; Invitrogen, Waltham, MA, USA) for 1 h. Finally, the samples were mounted in Permount Mounting Medium (SP15-500, Fisher Scientific, Waltham, MA, USA) and photographed using an Axio Scan Z1 slide scanner (ZEISS).

2.8. Fibroblast Isolation and Cell Culture

Primary cultured HDFs were obtained by circumcision surgery. Foreskin collection was approved by the Tri-Service General Hospital Institutional Review Board. Tissue samples were prepared as described by Rnjak et al. [35]. The separated cells were maintained in Dulbecco's modified Eagle medium (DMEM; Gibco, Waltham, MA, USA) supplemented with 10% fetal bovine serum (FBS) and 1% penicillin-streptomycin. All cell experiments were performed using primary cultured HDFs at passages 2–5.

2.9. HaCaT Cell Culture

The HaCaT immortal human keratinocyte cell line was purchased from CLS Cell Lines Service GmbH (#300493; Eppelheim Germany). HaCaT cells were cultured in DMEM (3.7 g/L NaHCO_3 and 110 mg/L sodium pyruvate) (Gibco) supplemented with 10% FBS, 1% penicillin-streptomycin, and 2 mM L-glutamine in a CO_2 incubator at 37 $^\circ\text{C}$.

2.10. Cell Migration

A culture insert (#80209; ibidi GmbH, Gräfelfing, Germany) was placed in each well of a 24-well culture plate. For the SF group, the inside bottom area of the culture insert was coated in aqueous solution of SF (0.1 $\mu\text{g}/\text{cm}^2$). After evaporation, a 75% ethanol solution was added for to induce β -sheet formation [24]. The control group culture insert was not treated with SF coating. Primary HDFs and HaCaT cells were maintained in the culture medium with 1% FBS for 24 h and were seeded outside the culture-inserts at a density of 1×10^6 cells per well. Once all the cells were attached to the plate, the cell-migrating area was observed and recorded at 24, 72, and 168 h, after removing the culture-inserts.

2.11. Western Blot

Primary cultures of HDFs (2×10^5 cells per well) were seeded in a six-well culture plate coated with or without SF. After treatment for 168 h, the cultured cells were harvested directly using a radioimmunoprecipitation assay lysis buffer system (sc-24948; Santa Cruz Biotechnology). The rat wound tissue was homogenized in lysis buffer. Cell and tissue protein concentrations were determined using a Coomassie protein assay reagent (Thermo Fisher Scientific, Waltham, MA, USA). For sodium dodecyl sulfate-polyacrylamide gel electrophoresis, the protein samples (15 μ g) were loaded on 10% SDS-PAGE gel and transferred to an Immobilon-E polyvinylidene fluoride membrane (Merck Millipore, Burlington, MA, USA) by electroblotting. The membranes were incubated with the primary antibodies mentioned above (Section 2.6). Other primary antibodies included rabbit anti-p-mTOR, rabbit anti-mTOR, rabbit anti-p-NF- κ B, rabbit anti-NF- κ B, mouse anti-nuclear factor of kappa light polypeptide gene enhancer in B-cells inhibitor, alpha ($\text{I}\kappa\text{B}\alpha$), rabbit anti-phosphorylated-extracellular signal-regulated kinase 1/2 (ERK1/2), rabbit anti-ERK1/2, rabbit anti-phosphorylated-c-Jun N-terminal kinase (JNK), rabbit anti-JNK, rabbit anti-phosphorylated-c-Jun, rabbit anti-c-Jun (#5536, #2972, #3033, #8242, #4814, #4370, #46955, #4668, #9252, #9261, #9165, respectively; 1:1000, Cell Signaling Technology, Inc., Danvers, MA, USA), mouse anti-phosphorylated- $\text{I}\kappa\text{B}\alpha$, mouse anti-glyceraldehyde 3-phosphate dehydrogenase (GAPDH), mouse anti- α -actinin (sc-8404, sc-32233, sc-17829, respectively; 1:1000; Santa Cruz Biotechnology). The following secondary antibodies were used: goat anti-rabbit IgG antibody, mouse IgG antibody (GTX213110-01 and GTX213111-01, respectively; 1:1000; GeneTex). Protein signals from the membranes were detected with Amersham ECL reagent (RPN2106; Cytiva, Marlborough, MA, USA) using a chemiluminescent imaging and analysis system (MiniChemi 610; Sage Creation Science, Beijing, China). ImageJ software was used to detect the protein signal values.

2.12. Statistical Analysis

Statistical analyses were performed using GraphPad Prism 8 software (GraphPad Software, Inc., San Diego, CA, USA). All data are expressed as the mean \pm standard error of the mean. Significant differences between groups were analyzed using the one-tailed paired *t*-test. Statistical significance was set at $p < 0.05$.

3. Results

3.1. Preparation and Analysis of Ethanol-Treated LSFDF

We used LSFDF treated with 75% ethanol for the animal study (Figure 1A). The micro characterization including scanning electron microscopy image of LSFDF was showed in our previously published paper [19]. For the CD spectra of SF structure determination, we measured SF with or without 75% ethanol treatment. The secondary structure of the untreated SF coating is represented by two peaks between 208–230 nm and the sloping ellipticity between 230–240 nm, while SF treated with 75% ethanol showed a simple curve between 208–230 nm (Figure 1B). Our investigation showed that SF treated with 75% ethanol had more β -sheets than untreated SF coatings, in accordance with previous research [36–39].

3.2. β -Sheet LSFDF Promoted *In Vivo* Tissue Regeneration

The *in vivo* wound closure rate was evaluated (Figure 2) to investigate whether LSFDF promoted wound healing. Two burn wounds were created on each rat's dorsal skin and debrided the next day. One of the burn wounds on each rat was treated with β -sheet LSFDFs after debridement, while the other wound, treated with medical gauze, served as the control. Notably, the LSFDF group had minor wounds on day 10 compared with the control group (Figure 2A). Furthermore, the wound healing rate in the LSFDF group was increased by 12% vs. the control group ($p < 0.05$) (Figure 2B). However, there was no significant difference in wound contraction between the LSFDF and control groups on days 3 and 7 (Figure 2). In summary, LSFDF promoted burn wound repair in the late phase of wound healing, known as the proliferation phase.

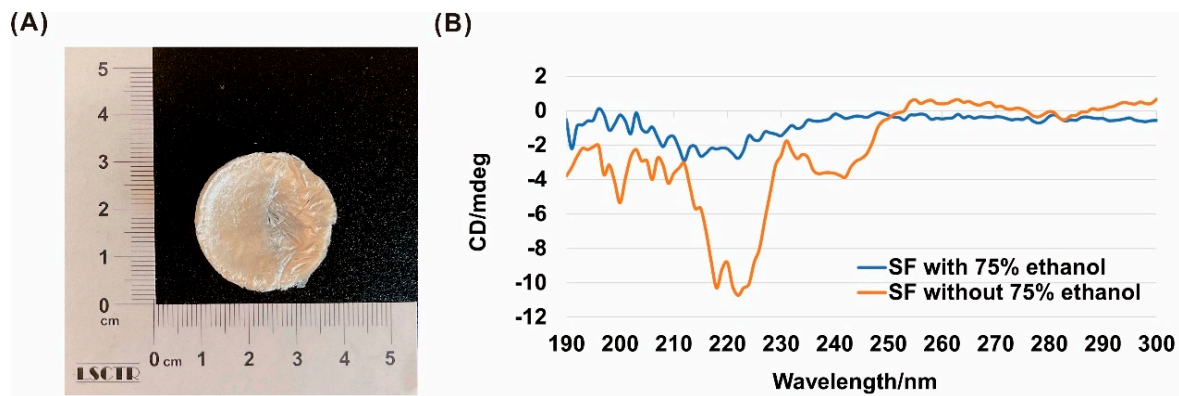


Figure 1. (A) Lyophilized silk fibroin dressing (LSFD) for the in vivo study; (B) circular dichroism (CD) spectra of SF treated with or without 75% ethanol.

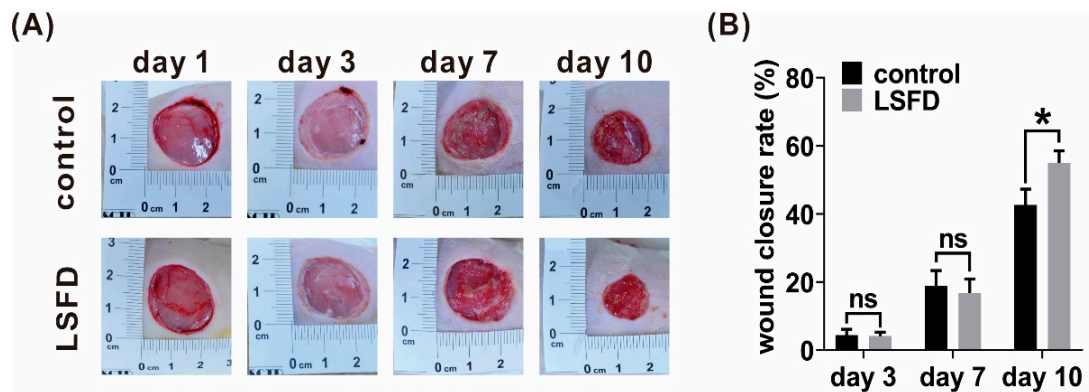


Figure 2. In vivo wound repair evaluation of β -sheet lyophilized silk fibroin dressing (LSFD)-treated burn injuries in rats. (A) The photographic appearance of burn wounds in β -sheet LSFDF and control groups on day 1, 3, 7, and 10 post-wounding. All animals received wound debridement on day 1. (B) Quantitative representation of the wound closure rate. Data are presented as the mean \pm standard error of the mean ($n = 7$; * $p < 0.05$, ns: not significant).

3.3. β -Sheet LSFDF Accelerated Re-Epithelialization and Granulation Formation in Burn Wounds

To determine whether β -sheet LSFDFs accelerate re-epithelialization and granulation formation, day-10 wound tissue sections were analyzed using histological staining. The results of H&E staining showed a significant increase in the re-epithelialized distance in the LSFDF group at day 10 vs. the control group. As for granulation tissue formation, a significantly thicker dermis was observed at day 10 in the LSFDF group compared with the control group (Figure 3A). K14, a type of structural filament, is a biomarker of the epithelial tongue during re-epithelialization [40]. Thus, epithelial tongues were detected using a K14-immunofluorescence assay. The LSFDF group showed a significantly longer distance of K14-staining area at day 10 vs. the control (Figure 3B). Collagen deposition is an essential foundational healing process during granulation tissue formation [41]. The collagen density on day 10 was significantly higher in the LSFDF group than in the control group (Figure 3C). Therefore, β -sheet LSFDF induced re-epithelialization and granulation formation during the proliferation phase of cutaneous wound healing.

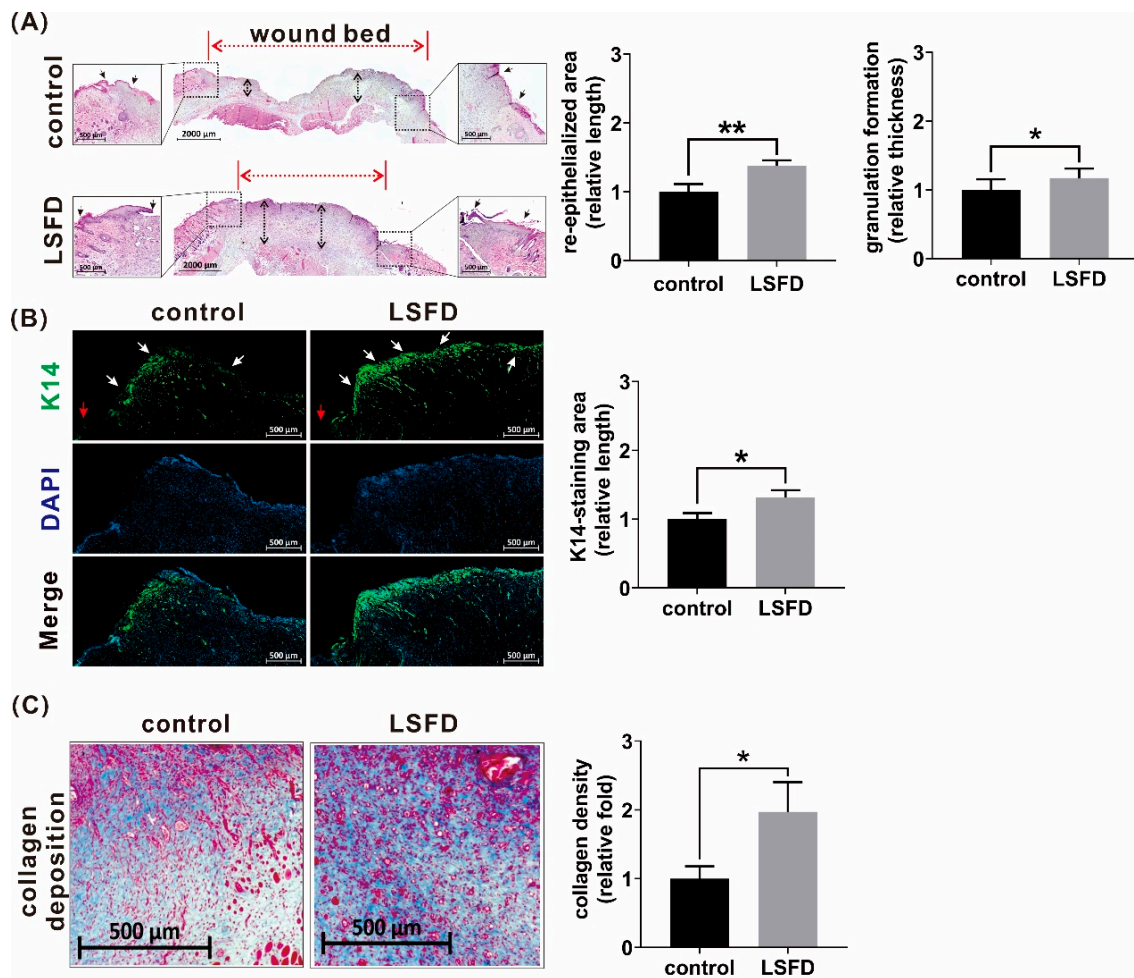


Figure 3. Histological characterization of rat burn wounds. (A) Hematoxylin and eosin staining of β -sheet LSF D-treated and control group tissue at day 10 post-wounding, showing the length of the re-epithelialized area and the thickness of the granulation tissue formation area. Black arrows: the distance from the original wound edges to re-epithelialized edges; black dashed arrows: granulation thickness; red dashed arrows: wound bed. (B) K14-immunofluorescence staining of epithelial tongues at day 10 post-wounding. White arrows: epithelial tongue area; red arrows: original wound edges; DAPI, 4',6-diamidino-2-phenylindole (C) Masson's Trichrome staining showing collagen deposition in rat skin at day 10 post-wounding. Quantitative data are presented as the mean \pm standard error of the mean ($n = 6$; * $p < 0.05$, ** $p < 0.01$).

3.4. β -Sheet SF Promoted *In Vitro* Migration of HDFs and HaCaT Keratinocytes

The effect of β -sheet LSF D on re-epithelialization and granulation formation during wound repair was confirmed. This indicates that keratinocytes and fibroblasts are attracted to the wound bed during tissue regeneration [42]. We investigated whether SF accelerated cell migration. To verify the cell recruitment abilities of SF, we used primary cultured HDFs and HaCaT keratinocytes. Fibroblasts in the SF-treated group showed a larger migrating area than the control group fibroblasts at 24, 72, and 168 h (Figure 4A), whereas SF-treated HaCaT keratinocytes only differed significantly from the control group at 72 h (Figure 4B). The tendency of SF to promote fibroblast migration was thus proven *in vitro*. We subsequently focused on granulation tissue formation *in vivo* and fibroblasts *in vitro*.

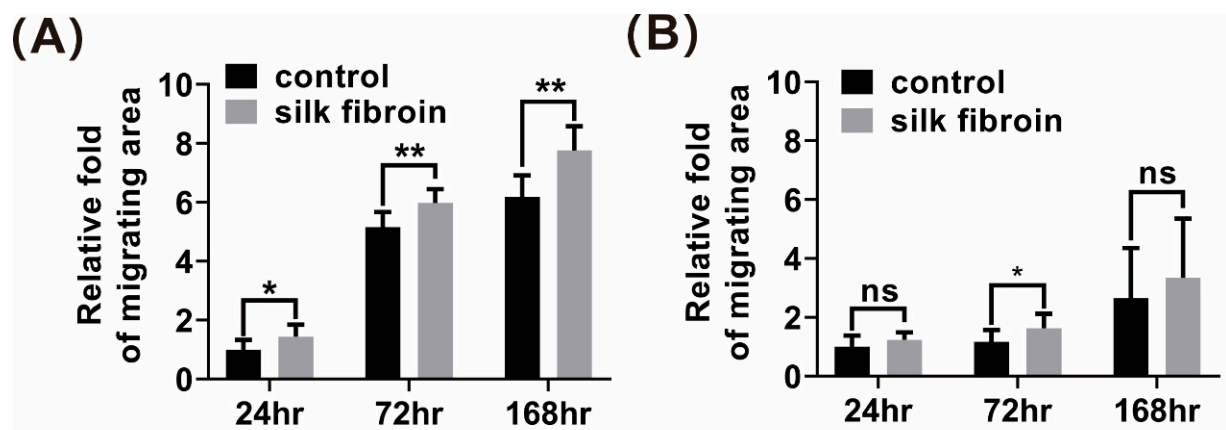


Figure 4. Influence of β -sheet silk fibroin on in vitro cell migration, expressed as the relative fold change in the migrating area of (A) human dermal fibroblasts and (B) HaCaT keratinocytes. Data are presented as the mean \pm standard error of the mean ($n = 4$; * $p < 0.05$, ** $p < 0.01$, ns: not significant).

3.5. β -Sheet LSFDF Promoted ECM Protein Expression in Rat Dermis

Collagen and other ECM proteins are responsible for granulation tissue formation in the dermis [43,44]. Our data showed that β -sheet LSFDF promoted collagen deposition in the rat dermis (Section 3.3; Figure 3C). We further investigated whether β -sheet LSFDF reconstructs dermal tissue by promoting several components of ECM proteins. IHC staining showed a significant increase in type III collagen, type I collagen, and FN expression in the LSFDF group at day 10 post-wounding vs. the control group (Figure 5A,B,D, respectively); vitronectin expression was not significantly different from the control group (Figure 5C). It is evident that β -sheet LSFDF promoted cutaneous regeneration partially by modulating the protein composition of the ECM.

3.6. Potential Mechanisms of β -Sheet LSFDF Related to Cell Adhesion Molecules

Previous studies demonstrated that soluble SF treatment in fibroblasts could significantly increase the gene expression of cell adhesion molecules, mTOR, and NF- κ B signaling pathways, which are involved in environmental information processing and promote cell migration [26]. Furthermore, human mammary gland and mink lung epithelial cell lines treated with soluble SF showed elevated expression of ERK1/2, JNK, and c-Jun, which are related to cell migration [45]. However, the mechanism by which β -sheet SF promotes fibroblast migration remains unknown and requires reliable evaluation in animal models. Because Western blotting of the homogenized wound bed tissue on day 10 showed no significant correlations between the phosphorylation of mTOR, NF- κ B, I κ B α , ERK1/2, JNK, and c-Jun between the LSFDF and control group (Figure 6), therefore we focused on the connection between ECM proteins and integrins during β -sheet SF treatment to explore other potential mechanisms. Our tissue section staining showed the upregulation of ECM proteins in the LSFDF group (Figure 5). Because integrins are ECM protein-binding receptors in cell adhesion molecules, they respond to cell motility and the actin cytoskeleton during wound repair [46]. Considering our observations, we hypothesize that SF may partially modulate integrin activity during dermal reconstruction.

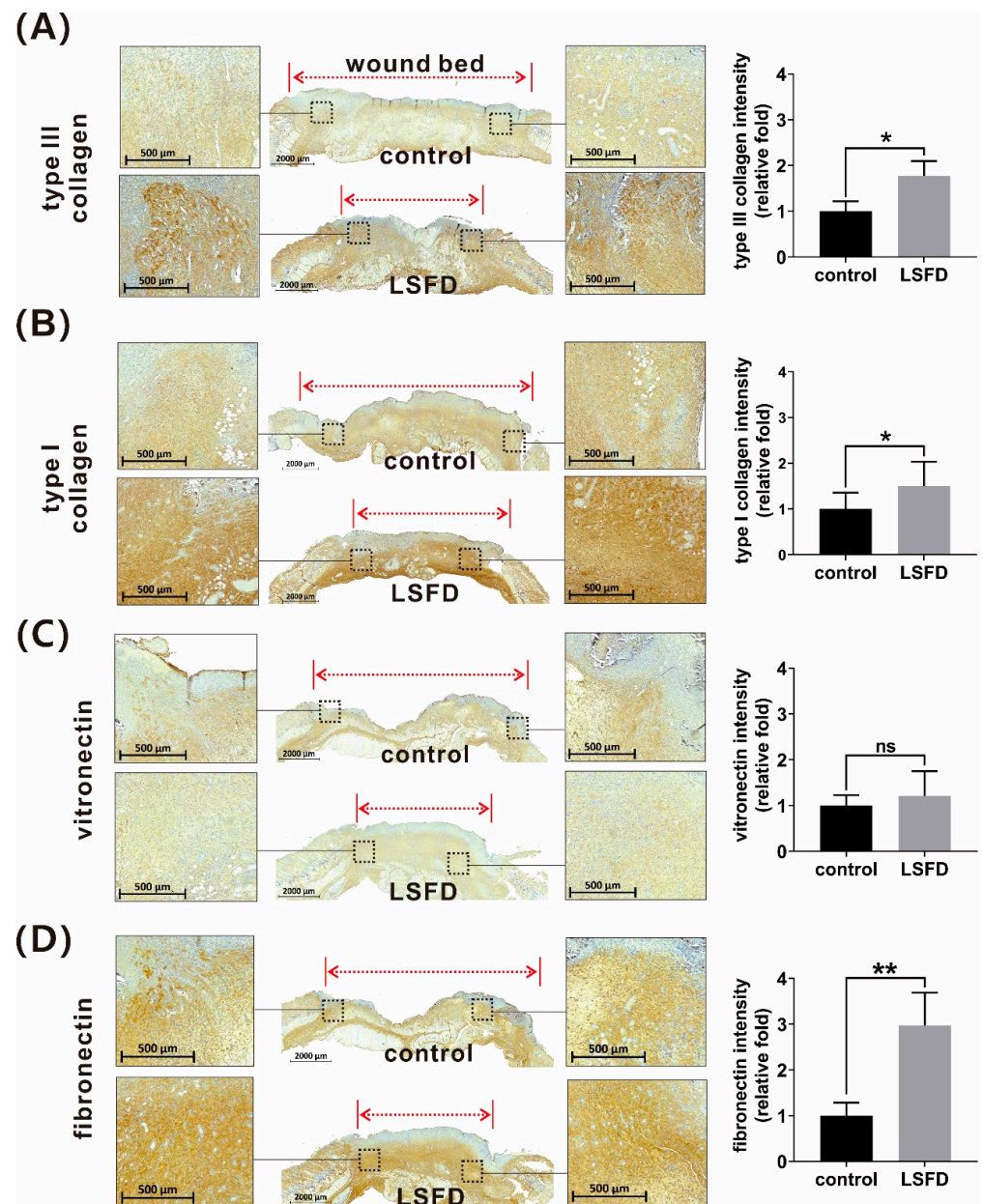


Figure 5. Immunohistochemistry staining and quantitative data of (A) type III collagen, (B) type I collagen, (C) vitronectin, (D) fibronectin rat tissue sections of the β -sheet lyophilized silk fibroin dressing (LSFDF)-treated group and the control group. All quantitative representations show the relative fold difference in ECM protein expression between the β -sheet LSFDF-treated group and the control group. Data are presented as the mean \pm standard error of the mean ($n = 6$; * $p < 0.05$, ** $p < 0.01$, ns: not significant).

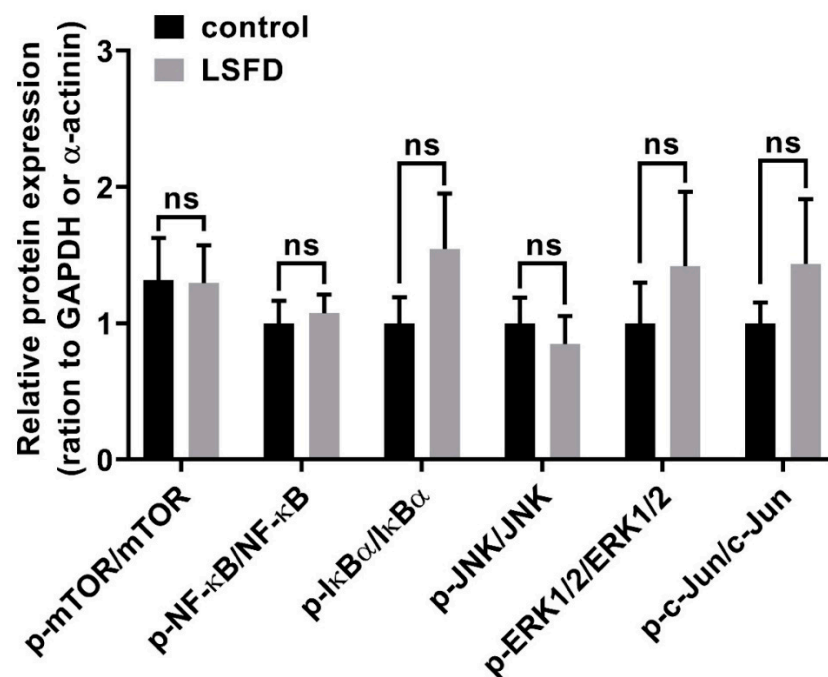


Figure 6. Western blot analysis data showing the relative protein expression in the wound bed at day 10 post-wounding in the control group and β -sheet LSFDF-treated group. GAPDH, glyceraldehyde 3-phosphate dehydrogenase I κ B α , nuclear factor of kappa light polypeptide gene enhancer in B-cells inhibitor, alpha; JNK, c-Jun N-terminal kinase; mTOR, mechanistic target of rapamycin; NF- κ B, nuclear factor kappa B; p indicates the phosphorylated protein. Data are presented as the mean \pm standard error of the mean ($n = 7$; ns: not significant).

3.7. β -Sheet LSFDF Modulated ECM-Specific Integrin Expression in Rat Dermis

Considering our targeted ECM proteins, specific integrins for collagen (integrin $\alpha 1$, $\alpha 2$, and $\beta 1$), vitronectin, and FN (integrin $\alpha 5$, αv , $\beta 1$, and $\beta 3$) were evaluated using IHC staining. Notably, the β -sheet LSFDF-treated group showed an increase in integrin $\alpha 1$, $\alpha 5$, $\beta 1$, and $\beta 3$ expression at day 10 (Figure 7A,C,E,F). However, there was no significant difference in integrin $\alpha 2$ and αv expression between the LSFDF and control groups (Figure 7B,D). Based on these observations, we inferred that SF may modulate cell adhesion molecules by topically facilitating integrin expression during dermal regeneration in burn wound healing.

3.8. β -Sheet LSFDF Increased Fibroblast Differentiation and MMP-12 Activity

The downstream functions of integrin include the regulation of the cytoskeleton and MMPs, which, respectively, are involved in fibroblast differentiation and cell motility [47]. The fibroblast differentiation marker, α -SMA, has been shown to modulate wound contraction [48]. MMPs can specifically degrade ECM proteins and promote cell motility [49]. We speculated that β -sheet LSFDF may modulate α -SMA and MMPs in the dermal layer network during burn wound healing. IHC staining and the *t*-test analysis indicated a significant difference in α -SMA and MMP-12 expression between the β -sheet LSFDF-treated group and the control group. However, there were no significant differences on day 10 between the two groups in the expression of MMP-1 and MMP-13 in granulation tissue (Figure 8).

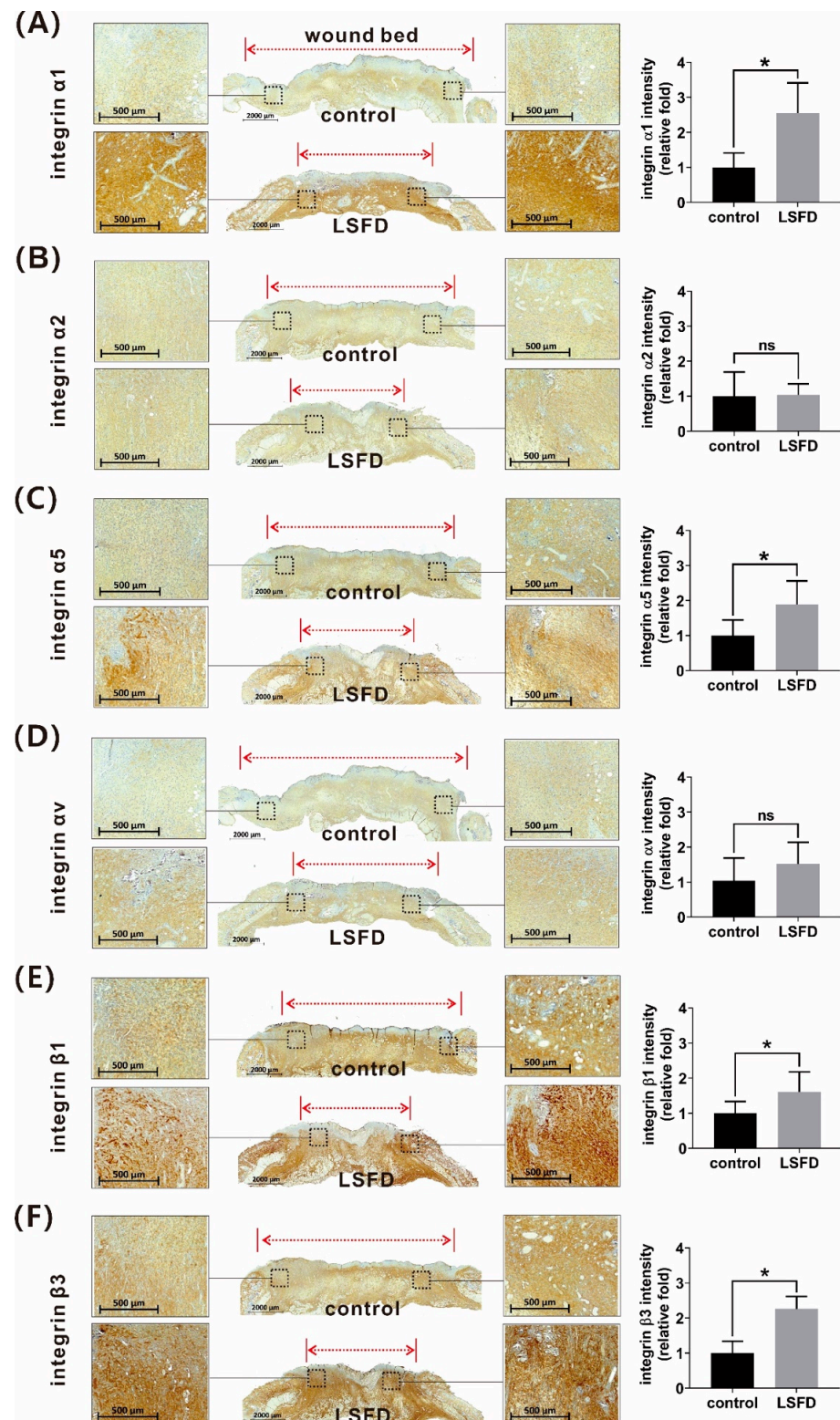


Figure 7. Immunohistochemistry staining and quantitative representations of the relative fold difference in the expression of different integrins in rat burn wounds treated with β -sheet lyophilized silk fibroin dressing (LSFD) and untreated burn wounds (control); (A) integrin $\alpha 1$; (B) integrin $\alpha 2$; (C) integrin $\alpha 5$; (D) integrin $\alpha \nu$; (E) integrin $\beta 1$; (F) integrin $\beta 3$. Data are presented as the mean \pm standard error of the mean ($n = 6$; * $p < 0.05$).

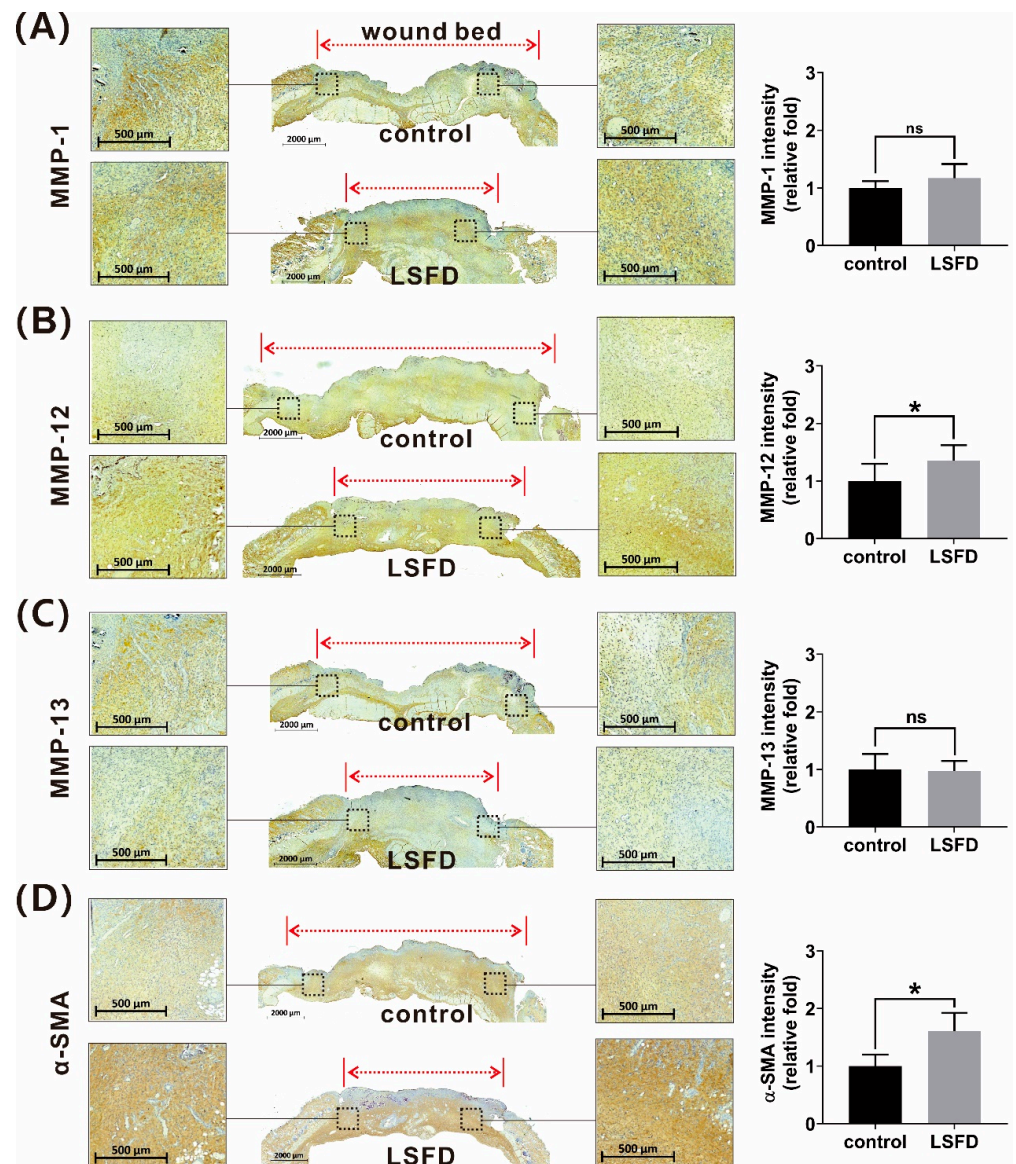


Figure 8. Immunohistochemistry staining of (A) matrix metalloproteinase-1 (MMP-1), (B) MMP-12, (C) MMP-13, and (D) α -smooth muscle actin (α -SMA) in day-10 tissue sections of untreated burn wounds (control) and burn wounds treated with β -sheet lyophilized silk fibroin dressing (LSFD). Quantitative representations show the relative fold difference in integrin and MMP expression between the LSFDF-treated group and the control group. Data are presented as the mean \pm standard error of the mean ($n = 6$; ns: not significant).

3.9. β -Sheet SF Stimulated In Vitro Expression of Integrin β 1 and ECM Proteins in HDFs

To evaluate integrin and ECM protein expression in β -sheet SF-treated burn wounds, we utilized primary cultured HDFs to explore the mechanism of cell migration. HDFs treated with β -sheet SF exhibited increased expression of FN and type III collagen, but without the modulation of type I collagen and MMP-12. Additionally, β -sheet SF further promoted the expression of integrin β 1, but not integrin α 1, α 5, β 3, and α -SMA (Figure 9A). Our in vitro results indicate that β -sheet SF specifically promoted the expression of FN, type III collagen, and integrin β 1 (Figure 9B).

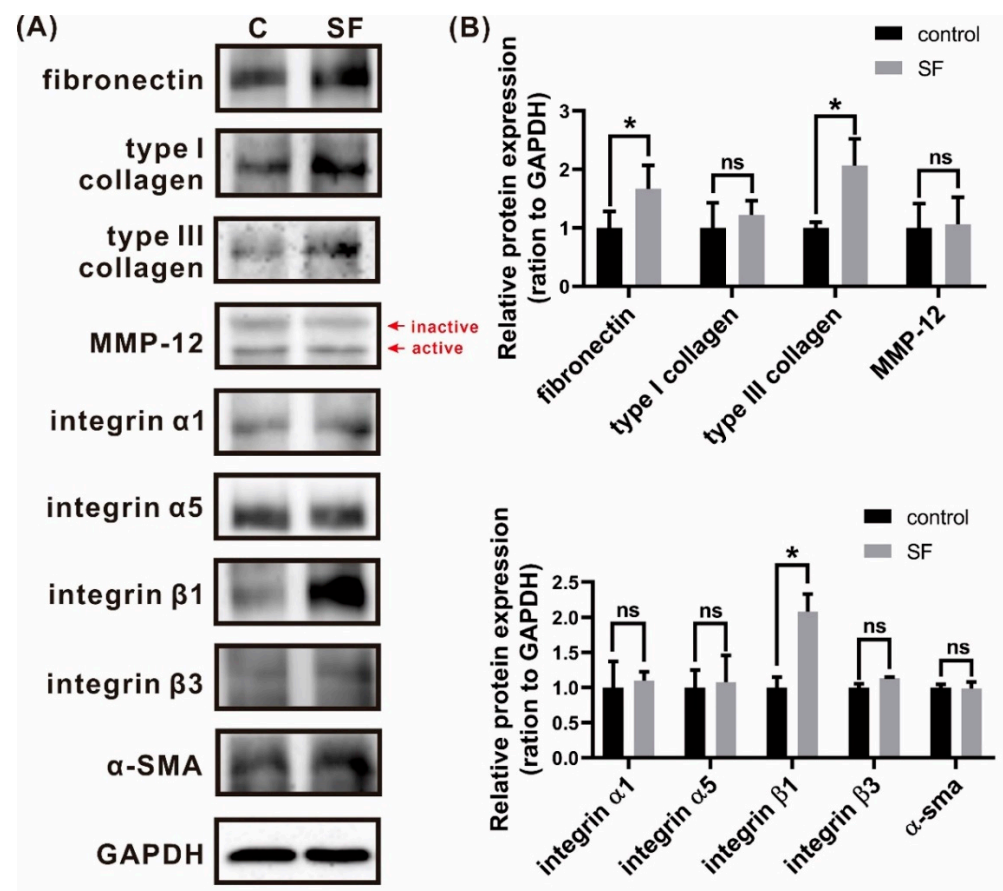


Figure 9. The protein expression in control and SF (silk fibroin) groups at 168 h were detected using Western blot analysis. (A) Fibronectin, type I collagen, type III collagen, MMP-12, integrin α 1, α 2, β 1, β 3, and α -SMA. (B) Quantitative representations showed the relative expression in the control and SF groups. Data are presented as the mean \pm standard error. * $p < 0.05$, ns: not significant). α -SMA, alpha-smooth muscle actin; GAPDH, glyceraldehyde 3-phosphate dehydrogenase; MMP-12, matrix metalloproteinase-12.

4. Discussion

As a biomaterial with stable physical and chemical properties, insoluble SF in β -sheet form has been developed into multiple types of wound dressings. In the past, studies rarely reported the underlying mechanism of β -sheet SF during cutaneous wound healing [15]. Here, we showed that LSFDF, which mainly consisted of β -sheet SF, promoted granulation tissue formation and re-epithelialization in an in vivo rat burn model and enhanced the motility of HDFs in vitro by increasing the expression of ECM proteins and integrin.

According to our animal experiments, LSFDF enhanced cutaneous wound healing during the proliferation phase, including granulation tissue formation and re-epithelialization. These two critical steps are essential for skin regeneration. Our results are consistent with those of previous studies that used SF dressing to improve wound healing [20,50,51]; however, previous studies did not focus on the influence of β -sheet SF. This study used 75% ethanol treatment to achieve an α -helix to β -sheet SF transition. Based on the findings from HDFs and HaCaT cell lines, we speculate that LSFDF promoted fibroblast migration and granulation tissue formation, which may assist in re-epithelialization through cell interactions.

Our results showed that β -sheet SF stimulated the expression of FN and type III collagen in HDFs in vitro and granulation tissue formation in vivo. FN and type III collagen, major ECM elements, are involved in cell migration and adhesion during tissue repair and correspond to specific integrins and MMPs [52–54]. Interestingly, type I collagen was

significantly upregulated *in vivo*, but not *in vitro*. As type III collagen can be converted into type I collagen during cutaneous healing [54], LSFDF may contribute to type I collagen synthesis by initially regulating type III collagen expression.

It is well known that MMPs secreted by dermal fibroblasts facilitate the migration of surrounding fibroblasts and keratinocytes [55,56], and that MMP-12 is responsible for the degradation of type I and III collagen [57,58]. In this study, LSFDF increased MMP-12 expression in granulation tissue; however, the *in vitro* results showed that β -sheet SF did not influence MMP-12 expression. As MMP-12 can be secreted by both fibroblasts and macrophages [59,60], LSFDF may modulate the macrophage response to MMP-12 secretion in the repaired wound bed. However, the interaction between β -sheet SF and macrophages requires verification.

Park et al. examined the gene levels of soluble SF-treated fibroblasts and observed that soluble SF moderated biomarkers of environmental information processing, including cell adhesion molecules [26]. Soluble SF further possesses an underlying mechanism involving phosphorylation kinases, including mTOR, NF- κ B, I κ B α , ERK1/2, JNK, and c-Jun [26,45,61]. However, significant phosphorylation levels of these kinases were not observed in the wound bed granulation tissue in this study. The divergence in SF treatment compared with previous research may be due to the SF forms, which differed from the β -sheet SF used in our experiments. These results indicate that soluble and insoluble SF may possess different migration mechanisms.

As for β -sheet forms of SF, Tan et al. demonstrated that insoluble SF induced integrin expression in endothelial cells, which participated in cell motility [29,62]. Therefore, we are interested in integrins, which belong to the receptors of ECM proteins and regulate cell migration and fibroblast differentiation [63,64]. Integrin α 5 β 1 and α v β 3 can bind with fibronectin [65] and play crucial roles in wound healing [66–68], while cell adhesion to collagen is mediated by integrin α 1 β 1 [69]. The β subunits form heterodimers with α integrins that can promote cell migration, which has been reported to participate in the development of cancer [70,71], the immune system [72], and in tissue repair [73,74]. β 1 knockout in fibroblasts reduced cell functions such as cell adhesion, spread, differentiation, expression of collagen and connective tissue growth factor, cutaneous wound closure, and ECM deposition [74]. Interestingly, α 1, α 5, β 1, and β 3 subunits were significantly upregulated in our *in vivo* study, while only the β 1 subunit was upregulated in HDFs *in vitro*. Additionally, LSFDF activated the expression of α -SMA, a biomarker of fibroblast differentiation, *in vivo*, but not *in vitro*. The inconsistency between the *in vivo* and *in vitro* results may be due to the complexity of the microenvironment during wound healing, which could influence α 1, α 5, and β 3 subunits and regulate fibroblast differentiation. The detailed working mechanisms of soluble and insoluble SF may be another issue for further investigation.

Our *in vivo* and *in vitro* results showed that LSFDF is beneficial for tissue regeneration. Besides, LSFDF is an ideal matrix for bringing small molecules or substances with weak mechanical properties to the living body, such as a gene delivery system for bone regeneration [75]. Moreover, the β -sheet form SF scaffold also could also provide a cancer cell migration system for studying cancer metastasis [76]. There were many kinds of SF wound dressing developed in the labs; however, the clinical trials of LSFDF are still lacking [77]. Until 2017, Zhang et al. verified that silk fibroin film, compared with commercial wound dressing, elevated wound healing in a randomized controlled clinical trial [78]. Therefore, the healing effect of LSFDF under ethanol treatment should be more validated in clinical trials.

Because SF possesses good mechanical strength, is non-cytotoxic, and does not cause inflammation and skin sensitivity, it is very suitable as a biomaterial for wound dressing [15]. The porosity of LSFDFs facilitates moisture absorption [79], allowing the burn wound exudate to be readily absorbed. Our animal experiments have also shown that LSFDF can keep the wound bed moist while not sticking to the wound, creating a favorable microenvironment for wound healing. Studies have indicated that the degradation rate

of silk with high β -sheet content is low [80], thus it maintains a stable structure on the wound bed. Hydrogel dressings or other easily degraded biological materials lack this property. LSFDF produced by lyophilization and ethanol treatment can be easily prepared on a large scale. However, after ethanol-treated SF is dried at room temperature, the texture becomes brittle [81]. This problem needs to be addressed in future studies. Fortunately, the mechanical properties of the β -sheet SF material can be adjusted by applying post-processing technologies [82]. By combining with other materials or adjusting the processing method, the softness and flexibility of the dressing can be improved to meet clinical requirements [83].

There are some limitations in this study. Because many commercial antibodies can be used in rats for biomolecular mechanism research, we chose rats for this animal experiment, which is also the species chosen by many scholars for animal studies of wound healing. However, the anatomical structure of rat skin is partially different from human skin, and the wound area that can be created in a rat is limited. Therefore, the severity of burns in rats is challenging to be categorized with the general scald grading of humans directly, and the current conclusion cannot be directly inferred to human skin and to more extensive wounds. Compared with other species, porcine skin is structurally closest to humans [84]. Hence, LSFDF should be investigated in porcine models for future preclinical animal studies.

In conclusion, this study demonstrated that β -sheet SF increased dermal fibroblast migration and upregulated the protein expression of ECM (fibronectin and type III collagen) and integrin $\beta 1$ subunit. This may promote granulation tissue formation, increase wound re-epithelialization, and finally improve burn wound healing (Figure 10). Our results suggest that LSFDF is a potential therapeutic strategy for promoting wound repair and regeneration. LSFDF could potentially be combined with anti-inflammatory materials, growth factors, or antibiotic reagents to develop various novel dressings with ideal qualities for tissue regeneration.

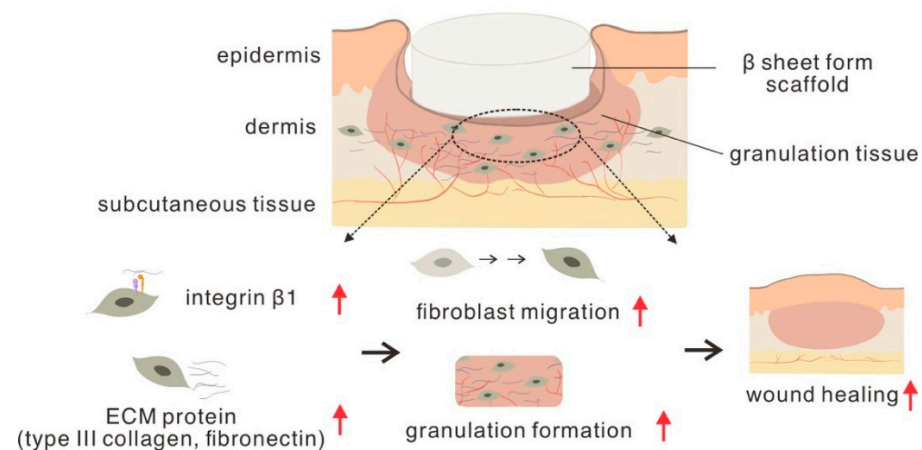


Figure 10. Schematic illustration of the summary in this study.

Author Contributions: Conceptualization, Y.-W.W. and J.-H.C.; methodology, K.-C.C. and C.-T.C.; software, K.-C.C. and C.-T.C.; validation, Y.-W.W. and J.-H.C.; formal analysis, K.-C.C. and C.-T.C.; investigation, K.-C.C., C.-T.C. and M.-C.L.; resources, Y.-W.W. and C.-T.C.; data curation, K.-C.C. and C.-T.C.; writing—original draft preparation, K.-C.C., C.-C.W., S.-I.H. and C.-C.W.; writing—review and editing, Y.-W.W. and J.-H.C.; visualization, K.-C.C. and C.-T.C.; supervision, Y.-W.W.; project administration, Y.-W.W.; funding acquisition, Y.-W.W. and C.-T.C. All authors have read and agreed to the published version of the manuscript.

Funding: This research was funded by grants from the Tri-Service General Hospital Penghu Branch, National Defense Medical Center (TSGH-PH-D-110009) and the Ministry of National Defense, (MND-MAB-110-047), Taiwan.

Acknowledgments: The authors would like to thank the Animal Center and Instrument Center of National Defense Medical Center and the Medical Research Office of the Tri-Service General Hospital for their support in instrument use and animal care.

Conflicts of Interest: The authors declare no conflict of interest.

References

1. Mason, S.A.; Nathens, A.B.; Byrne, J.P.; Diong, C.; Fowler, R.A.; Karanicolas, P.J.; Moineddin, R.; Jeschke, M.G. Increased Rate of Long-term Mortality Among Burn Survivors: A Population-based Matched Cohort Study. *Ann. Surg.* **2019**, *269*, 1192–1199. [[CrossRef](#)]
2. Rezvani Ghomi, E.; Khalili, S.; Nouri Khorasani, S.; Esmaeely Neisiany, R.; Ramakrishna, S. Wound dressings: Current advances and future directions. *J. Appl. Polym. Sci.* **2019**, *136*, 47738. [[CrossRef](#)]
3. Piraino, F.; Selimovic, S. A Current View of Functional Biomaterials for Wound Care, Molecular and Cellular Therapies. *Biomed. Res. Int.* **2015**, *2015*, 403801. [[CrossRef](#)]
4. Wu, J.; Xiao, Z.; Chen, A.; He, H.; He, C.; Shuai, X.; Li, X.; Chen, S.; Zhang, Y.; Ren, B.; et al. Sulfated zwitterionic poly(sulfobetaine methacrylate) hydrogels promote complete skin regeneration. *Acta Biomater.* **2018**, *71*, 293–305. [[CrossRef](#)]
5. Zhu, Y.; Ma, Z.; Kong, L.; He, Y.; Chan, H.F.; Li, H. Modulation of macrophages by bioactive glass/sodium alginate hydrogel is crucial in skin regeneration enhancement. *Biomaterials* **2020**, *256*, 120216. [[CrossRef](#)]
6. Nguyen, T.P.; Nguyen, Q.V.; Nguyen, V.H.; Le, T.H.; Huynh, V.Q.N.; Vo, D.N.; Trinh, Q.T.; Kim, S.Y.; Le, Q.V. Silk Fibroin-Based Biomaterials for Biomedical Applications: A Review. *Polymers* **2019**, *11*, 1933. [[CrossRef](#)]
7. Zhou, C.Z.; Confalonieri, F.; Jacquet, M.; Perasso, R.; Li, Z.G.; Janin, J. Silk fibroin: Structural implications of a remarkable amino acid sequence. *Proteins* **2001**, *44*, 119–122. [[CrossRef](#)]
8. Sheng, X.; Fan, L.; He, C.; Zhang, K.; Mo, X.; Wang, H. Vitamin E-loaded silk fibroin nanofibrous mats fabricated by green process for skin care application. *Int. J. Biol. Macromol.* **2013**, *56*, 49–56. [[CrossRef](#)]
9. Madden, P.W.; Klyubin, I.; Ahearne, M.J. Silk fibroin safety in the eye: A review that highlights a concern. *BMJ Open Ophthalmol.* **2020**, *5*, e000510. [[CrossRef](#)]
10. Zhang, Y.; Lu, L.; Chen, Y.; Wang, J.; Chen, Y.; Mao, C.; Yang, M. Polydopamine modification of silk fibroin membranes significantly promotes their wound healing effect. *Biomater. Sci.* **2019**, *7*, 5232–5237. [[CrossRef](#)]
11. Cheng, G.; Davoudi, Z.; Xing, X.; Yu, X.; Cheng, X.; Li, Z.; Deng, H.; Wang, Q. Advanced Silk Fibroin Biomaterials for Cartilage Regeneration. *ACS Biomater. Sci. Eng.* **2018**, *4*, 2704–2715. [[CrossRef](#)] [[PubMed](#)]
12. Li, Y.; Yang, Y.; Yang, L.; Zeng, Y.; Gao, X.; Xu, H. Poly(ethylene glycol)-modified silk fibroin membrane as a carrier for limbal epithelial stem cell transplantation in a rabbit LSCD model. *Stem Cell Res.* **2017**, *8*, 256. [[CrossRef](#)] [[PubMed](#)]
13. Sun, W.; Gregory, D.A.; Tomeh, M.A.; Zhao, X. Silk Fibroin as a Functional Biomaterial for Tissue Engineering. *Int. J. Mol. Sci.* **2021**, *22*, 1499. [[CrossRef](#)]
14. Lee, O.J.; Sultan, M.; Hong, H.; Lee, Y.J.; Lee, J.S.; Lee, H.; Kim, S.H.; Park, C.H. Recent advances in fluorescent silk fibroin. *Front. Mater.* **2020**, *7*, 50. [[CrossRef](#)]
15. Kamalathevan, P.; Ooi, P.S.; Loo, Y.L. Silk-Based Biomaterials in Cutaneous Wound Healing: A Systematic Review. *Adv. Ski. Wound Care* **2018**, *31*, 565–573. [[CrossRef](#)]
16. Kaewpirom, S.; Boonsang, S. Influence of alcohol treatments on properties of silk-fibroin-based films for highly optically transparent coating applications. *RSC Adv.* **2020**, *10*, 15913–15923. [[CrossRef](#)]
17. Zhang, Y.-Q.; Shen, W.-D.; Xiang, R.-L.; Zhuge, L.-J.; Gao, W.-J.; Wang, W.-B. Formation of silk fibroin nanoparticles in water-miscible organic solvent and their characterization. *J. Nanoparticle Res.* **2007**, *9*, 885–900. [[CrossRef](#)]
18. Bhardwaj, N.; Sow, W.T.; Devi, D.; Ng, K.W.; Mandal, B.B.; Cho, N.-J. Silk fibroin–keratin based 3D scaffolds as a dermal substitute for skin tissue engineering. *Integr. Biol.* **2015**, *7*, 53–63. [[CrossRef](#)]
19. Sartika, D.; Wang, C.-H.; Wang, D.-H.; Cherg, J.-H.; Chang, S.-J.; Fan, G.-Y.; Wang, Y.-W.; Lee, C.-H.; Hong, P.-D.; Wang, C.-C. Human adipose-derived mesenchymal stem cells-incorporated silk fibroin as a potential bio-scaffold in guiding bone regeneration. *Polymers* **2020**, *12*, 853. [[CrossRef](#)]
20. Zha, X.; Xiong, X.; Chen, C.; Li, Y.; Zhang, L.; Xie, H.; Jiang, Q. Usnic-Acid-Functionalized Silk Fibroin Composite Scaffolds for Cutaneous Wounds Healing. *Macromol. Biosci.* **2021**, *21*, e2000361. [[CrossRef](#)]
21. Johari, N.; Moroni, L.; Samadikuchaksaraei, A. Tuning the conformation and mechanical properties of silk fibroin hydrogels. *Eur. Polym. J.* **2020**, *134*, 109842. [[CrossRef](#)]
22. Kundu, B.; Rajkhowa, R.; Kundu, S.C.; Wang, X. Silk fibroin biomaterials for tissue regenerations. *Adv. Drug Deliv. Rev.* **2013**, *65*, 457–470. [[CrossRef](#)]
23. Yu, L.M.; Liu, T.; Ma, Y.L.; Zhang, F.; Huang, Y.C.; Fan, Z.H. Fabrication of Silk-Hyaluronan Composite as a Potential Scaffold for Tissue Repair. *Front Bioeng. Biotechnol.* **2020**, *8*, 578988. [[CrossRef](#)] [[PubMed](#)]
24. Nogueira, G.M.; Rodas, A.C.; Leite, C.A.; Giles, C.; Higa, O.Z.; Polakiewicz, B.; Beppu, M.M. Preparation and characterization of ethanol-treated silk fibroin dense membranes for biomaterials application using waste silk fibers as raw material. *Bioresour. Technol.* **2010**, *101*, 8446–8451. [[CrossRef](#)] [[PubMed](#)]
25. Partlow, B.P.; Bagheri, M.; Harden, J.L.; Kaplan, D.L. Tyrosine Templating in the Self-Assembly and Crystallization of Silk Fibroin. *Biomacromolecules* **2016**, *17*, 3570–3579. [[CrossRef](#)] [[PubMed](#)]

26. Park, Y.R.; Sultan, M.T.; Park, H.J.; Lee, J.M.; Ju, H.W.; Lee, O.J.; Lee, D.J.; Kaplan, D.L.; Park, C.H. NF-kappaB signaling is key in the wound healing processes of silk fibroin. *Acta Biomater.* **2018**, *67*, 183–195. [CrossRef]
27. Koivisto, L.; Heino, J.; Hakkinen, L.; Larjava, H. Integrins in Wound Healing. *Adv. Wound Care* **2014**, *3*, 762–783. [CrossRef] [PubMed]
28. Jones, C.; Ehrlich, H.P. Fibroblast expression of alpha-smooth muscle actin, alpha2beta1 integrin and alphavbeta3 integrin: Influence of surface rigidity. *Exp. Mol. Pathol.* **2011**, *91*, 394–399. [CrossRef]
29. Tan, J.Y.; Wen, J.C.; Shi, W.H.; He, Q.; Zhu, L.; Liang, K.; Shao, Z.Z.; Yu, B. Effect of microtopographic structures of silk fibroin on endothelial cell behavior. *Mol. Med. Rep.* **2013**, *7*, 292–298. [CrossRef]
30. Bondar, B.; Fuchs, S.; Motta, A.; Migliaresi, C.; Kirkpatrick, C.J. Functionality of endothelial cells on silk fibroin nets: Comparative study of micro- and nanometric fibre size. *Biomaterials* **2008**, *29*, 561–572. [CrossRef]
31. Hong, H.; Seo, Y.B.; Kim, D.Y.; Lee, J.S.; Lee, Y.J.; Lee, H.; Ajiteru, O.; Sultan, M.T.; Lee, O.J.; Kim, S.H.; et al. Digital light processing 3D printed silk fibroin hydrogel for cartilage tissue engineering. *Biomaterials* **2020**, *232*, 119679. [CrossRef]
32. Li, Y.; Chen, M.; Zhou, W.; Gao, S.; Luo, X.; Peng, L.; Yan, J.; Wang, P.; Li, Q.; Zheng, Y.; et al. Cell-free 3D wet-electrospun PCL/silk fibroin/Sr(2+) scaffold promotes successful total meniscus regeneration in a rabbit model. *Acta Biomater.* **2020**, *113*, 196–209. [CrossRef]
33. Wang, C.H.; Chang, S.J.; Tzeng, Y.S.; Shih, Y.J.; Adrienne, C.; Chen, S.G.; Chen, T.M.; Dai, N.T.; Cherng, J.H. Enhanced wound-healing performance of a phyto-polysaccharide-enriched - a preclinical small and large animal study. *Int. Wound J.* **2017**, *14*, 1359–1369. [CrossRef] [PubMed]
34. Tavares Pereira Ddos, S.; Lima-Ribeiro, M.H.; de Pontes-Filho, N.T.; Carneiro-Leao, A.M.; Correia, M.T. Development of animal model for studying deep second-degree thermal burns. *J. Biomed. Biotechnol.* **2012**, *2012*, 460841. [CrossRef]
35. Rnjak, J.; Li, Z.; Maitz, P.K.; Wise, S.G.; Weiss, A.S. Primary human dermal fibroblast interactions with open weave three-dimensional scaffolds prepared from synthetic human elastin. *Biomaterials* **2009**, *30*, 6469–6477. [CrossRef]
36. Greenfield, N.; Fasman, G.D. Computed circular dichroism spectra for the evaluation of protein conformation. *Biochemistry* **1969**, *8*, 4108–4116. [CrossRef]
37. Wei, Y.; Thyparambil, A.A.; Latour, R.A. Protein helical structure determination using CD spectroscopy for solutions with strong background absorbance from 190 to 230nm. *Biochim. Biophys. Acta* **2014**, *1844*, 2331–2337. [CrossRef]
38. Yang, Y.; Shao, Z.; Chen, X.; Zhou, P. Optical spectroscopy to investigate the structure of regenerated Bombyx mori silk fibroin in solution. *Biomacromolecules* **2004**, *5*, 773–779. [CrossRef]
39. Midha, S.; Kumar, S.; Sharma, A.; Kaur, K.; Shi, X.; Naruphontjirakul, P.; Jones, J.R.; Ghosh, S. Silk fibroin-bioactive glass based advanced biomaterials: Towards patient-specific bone grafts. *Biomed. Mater.* **2018**, *13*, 055012. [CrossRef] [PubMed]
40. Gnyawali, S.C.; Barki, K.G.; Mathew-Steiner, S.S.; Dixith, S.; Vanzant, D.; Kim, J.; Dickerson, J.L.; Datta, S.; Powell, H.; Roy, S.; et al. High-resolution harmonics ultrasound imaging for non-invasive characterization of wound healing in a pre-clinical swine model. *PLoS ONE* **2015**, *10*, e0122327. [CrossRef] [PubMed]
41. Velnar, T.; Bailey, T.; Smrkolj, V. The wound healing process: An overview of the cellular and molecular mechanisms. *J. Int. Med. Res.* **2009**, *37*, 1528–1542. [CrossRef] [PubMed]
42. Wojtowicz, A.M.; Oliveira, S.; Carlson, M.W.; Zawadzka, A.; Rousseau, C.F.; Baksh, D. The importance of both fibroblasts and keratinocytes in a bilayered living cellular construct used in wound healing. *Wound Repair. Regen.* **2014**, *22*, 246–255. [CrossRef] [PubMed]
43. Volk, S.W.; Iqbal, S.A.; Bayat, A. Interactions of the Extracellular Matrix and Progenitor Cells in Cutaneous Wound Healing. *Adv. Wound Care* **2013**, *2*, 261–272. [CrossRef] [PubMed]
44. Xue, M.; Jackson, C.J. Extracellular Matrix Reorganization During Wound Healing and Its Impact on Abnormal Scarring. *Adv. Wound Care* **2015**, *4*, 119–136. [CrossRef] [PubMed]
45. Martinez-Mora, C.; Mrowiec, A.; Garcia-Vizcaino, E.M.; Alcaraz, A.; Cenis, J.L.; Nicolas, F.J. Fibroin and sericin from Bombyx mori silk stimulate cell migration through upregulation and phosphorylation of c-Jun. *PLoS ONE* **2012**, *7*, e42271. [CrossRef] [PubMed]
46. Cheng, F.; Eriksson, J.E. Intermediate Filaments and the Regulation of Cell Motility during Regeneration and Wound Healing. *Cold Spring Harb. Perspect. Biol.* **2017**, *9*, a022046. [CrossRef]
47. Sabino, F.; Auf dem Keller, U. Matrix metalloproteinases in impaired wound healing. *Met. Med.* **2015**, *2*, 1–8. [CrossRef]
48. Yeh, C.J.; Chen, C.C.; Leu, Y.L.; Lin, M.W.; Chiu, M.M.; Wang, S.H. The effects of artocarpin on wound healing: In vitro and in vivo studies. *Sci. Rep.* **2017**, *7*, 15599. [CrossRef]
49. Caley, M.P.; Martins, V.L.; O’Toole, E.A. Metalloproteinases and Wound Healing. *Adv. Wound Care* **2015**, *4*, 225–234. [CrossRef]
50. Rajput, M.; Mandal, M.; Anura, A.; Mukhopadhyay, A.; Subramanian, B.; Paul, R.R.; Chatterjee, J. Honey loaded silk fibroin 3D porous scaffold facilitates homeostatic full-thickness wound healing. *Materialia* **2020**, *12*, 100703. [CrossRef]
51. Baker, B.L.; Whitaker, W.L. Interference with wound healing by the local action of adrenocortical steroids. *Endocrinology* **1950**, *46*, 544–551. [CrossRef]
52. Larjava, H.; Koivisto, L.; Häkkinen, L. Keratinocyte interactions with fibronectin during wound healing. In *Madame Curie Bioscience Database*; 2013. Available online: <https://www.ncbi.nlm.nih.gov/books/NBK6391/> (accessed on 11 October 2021).
53. Tschumperlin, D.J. Fibroblasts and the ground they walk on. *Physiol. (Bethesda)* **2013**, *28*, 380–390. [CrossRef] [PubMed]

54. Li, W.; Fan, J.; Chen, M.; Guan, S.; Sawcer, D.; Bokoch, G.M.; Woodley, D.T. Mechanism of human dermal fibroblast migration driven by type I collagen and platelet-derived growth factor-BB. *Mol. Biol. Cell* **2004**, *15*, 294–309. [[CrossRef](#)] [[PubMed](#)]
55. Tracy, L.E.; Minasian, R.A.; Caterson, E.J. Extracellular Matrix and Dermal Fibroblast Function in the Healing Wound. *Adv. Wound Care* **2016**, *5*, 119–136. [[CrossRef](#)]
56. Chen, P.; Parks, W.C. Role of matrix metalloproteinases in epithelial migration. *J. Cell Biochem.* **2009**, *108*, 1233–1243. [[CrossRef](#)] [[PubMed](#)]
57. Jablonska-Trypuc, A.; Matejczyk, M.; Rosochacki, S. Matrix metalloproteinases (MMPs), the main extracellular matrix (ECM) enzymes in collagen degradation, as a target for anticancer drugs. *J. Enzym. Inhib. Med. Chem.* **2016**, *31*, 177–183. [[CrossRef](#)]
58. Van Doren, S.R. Matrix metalloproteinase interactions with collagen and elastin. *Matrix. Biol.* **2015**, *44–46*, 224–231. [[CrossRef](#)]
59. Chan, M.F.; Li, J.; Bertrand, A.; Casbon, A.J.; Lin, J.H.; Maltseva, I.; Werb, Z. Protective effects of matrix metalloproteinase-12 following corneal injury. *J. Cell Sci.* **2013**, *126*, 3948–3960. [[CrossRef](#)]
60. Aristorena, M.; Gallardo-Vara, E.; Vicen, M.; de Las Casas-Engel, M.; Ojeda-Fernandez, L.; Nieto, C.; Blanco, F.J.; Valbuena-Diez, A.C.; Botella, L.M.; Nachtigal, P.; et al. MMP-12, Secreted by Pro-Inflammatory Macrophages, Targets Endoglin in Human Macrophages and Endothelial Cells. *Int. J. Mol. Sci.* **2019**, *20*, 3107. [[CrossRef](#)]
61. Chon, J.W.; Kim, H.; Jeon, H.N.; Park, K.; Lee, K.G.; Yeo, J.H.; Kweon, H.; Lee, H.S.; Jo, Y.Y.; Park, Y.K. Silk fibroin hydrolysate inhibits osteoclastogenesis and induces apoptosis of osteoclasts derived from RAW 264.7 cells. *Int. J. Mol. Med.* **2012**, *30*, 1203–1210. [[CrossRef](#)]
62. Holly, S.P.; Larson, M.K.; Parise, L.V. Multiple roles of integrins in cell motility. *Exp. Cell Res.* **2000**, *261*, 69–74. [[CrossRef](#)]
63. Huang, C.; Fu, X.; Liu, J.; Qi, Y.; Li, S.; Wang, H. The involvement of integrin beta1 signaling in the migration and myofibroblastic differentiation of skin fibroblasts on anisotropic collagen-containing nanofibers. *Biomaterials* **2012**, *33*, 1791–1800. [[CrossRef](#)] [[PubMed](#)]
64. Zhao, X.K.; Cheng, Y.; Liang Cheng, M.; Yu, L.; Mu, M.; Li, H.; Liu, Y.; Zhang, B.; Yao, Y.; Guo, H.; et al. Focal Adhesion Kinase Regulates Fibroblast Migration via Integrin beta-1 and Plays a Central Role in Fibrosis. *Sci. Rep.* **2016**, *6*, 19276. [[CrossRef](#)]
65. Schnittert, J.; Bansal, R.; Storm, G.; Prakash, J. Integrins in wound healing, fibrosis and tumor stroma: High potential targets for therapeutics and drug delivery. *Adv Drug Deliv. Rev.* **2018**, *129*, 37–53. [[CrossRef](#)] [[PubMed](#)]
66. Van Bergen, T.; Zahn, G.; Caldirola, P.; Fsadni, M.; Caram-Lelham, N.; Vandewalle, E.; Moons, L.; Stalmans, I. Integrin alpha5beta1 Inhibition by CLT-28643 Reduces Postoperative Wound Healing in a Mouse Model of Glaucoma Filtration Surgery. *Invest. Ophthalmol. Vis. Sci.* **2016**, *57*, 6428–6439. [[CrossRef](#)] [[PubMed](#)]
67. Bi, J.J.; Yi, L. Effects of integrins and integrin alphavbeta3 inhibitor on angiogenesis in cerebral ischemic stroke. *J. Huazhong Univ. Sci. Technol. Med. Sci.* **2014**, *34*, 299–305. [[CrossRef](#)] [[PubMed](#)]
68. Racine-Samson, L.; Rockey, D.C.; Bissell, D.M. The role of alpha1beta1 integrin in wound contraction. A quantitative analysis of liver myofibroblasts in vivo and in primary culture. *J. Biol. Chem.* **1997**, *272*, 30911–30917. [[CrossRef](#)]
69. Hudson, S.V.; Dolin, C.E.; Poole, L.G.; Massey, V.L.; Wilkey, D.; Beier, J.I.; Merchant, M.L.; Frieboes, H.B.; Arteel, G.E. Modeling the Kinetics of Integrin Receptor Binding to Hepatic Extracellular Matrix Proteins. *Sci. Rep.* **2017**, *7*, 12444. [[CrossRef](#)]
70. Ramirez, N.E.; Zhang, Z.; Madamanchi, A.; Boyd, K.L.; O'Rear, L.D.; Nashabi, A.; Li, Z.; Dupont, W.D.; Zijlstra, A.; Zutter, M.M. The alpha(2)beta(1) integrin is a metastasis suppressor in mouse models and human cancer. *J. Clin. Invest.* **2011**, *121*, 226–237. [[CrossRef](#)]
71. Kovacheva, M.; Zepp, M.; Berger, S.; Berger, M.R. Conditional knockdown of integrin beta-3 reveals its involvement in osteolytic and soft tissue lesions of breast cancer skeletal metastasis. *J. Cancer Res. Clin. Oncol.* **2021**, *147*, 361–371. [[CrossRef](#)]
72. Fernandes, N.R.J.; Reilly, N.S.; Schrock, D.C.; Hocking, D.C.; Oakes, P.W.; Fowell, D.J. CD4(+) T Cell Interstitial Migration Controlled by Fibronectin in the Inflamed Skin. *Front Immunol.* **2020**, *11*, 1501. [[CrossRef](#)]
73. Oliveira, C.R.; Marqueti Rde, C.; Cominetti, M.R.; Vieira, E.S.; Ribeiro, J.U.; Pontes, C.L.; Borghi-Silva, A.; Selistre-de-Araujo, H.S. Effects of Blocking alphavbeta(3) integrin by a recombinant RGD disintegrin on remodeling of wound healing after induction of incisional hernia in rats. *Acta Cir. Bras.* **2014**, *29* (Suppl. 3), 6–13. [[CrossRef](#)]
74. Liu, S.; Xu, S.W.; Blumbach, K.; Eastwood, M.; Denton, C.P.; Eckes, B.; Krieg, T.; Abraham, D.J.; Leask, A. Expression of integrin beta1 by fibroblasts is required for tissue repair in vivo. *J. Cell Sci.* **2010**, *123*, 3674–3682. [[CrossRef](#)]
75. Zhang, Y.; Wu, C.; Luo, T.; Li, S.; Cheng, X.; Miron, R.J. Synthesis and inflammatory response of a novel silk fibroin scaffold containing BMP7 adenovirus for bone regeneration. *Bone* **2012**, *51*, 704–713. [[CrossRef](#)]
76. Kwon, H.; Kim, H.J.; Rice, W.L.; Subramanian, B.; Park, S.H.; Georgakoudi, I.; Kaplan, D.L. Development of an in vitro model to study the impact of BMP-2 on metastasis to bone. *J. Tissue Eng. Regen. Med.* **2010**, *4*, 590–599. [[CrossRef](#)]
77. SinghShera, S.; Das, N. Silk fibroin in effective wound dressing: An overview. *Int. J. Adv. Res.* **2019**, *7*, 68–72. [[CrossRef](#)]
78. Zhang, W.; Chen, L.; Chen, J.; Wang, L.; Gui, X.; Ran, J.; Xu, G.; Zhao, H.; Zeng, M.; Ji, J.; et al. Silk Fibroin Biomaterial Shows Safe and Effective Wound Healing in Animal Models and a Randomized Controlled Clinical Trial. *Adv. Healthc Mater.* **2017**, *6*, 1700121. [[CrossRef](#)]
79. Rnjak-Kovacina, J.; Wray, L.S.; Burke, K.A.; Torregrosa, T.; Golinski, J.M.; Huang, W.; Kaplan, D.L. Lyophilized Silk Sponges: A Versatile Biomaterial Platform for Soft Tissue Engineering. *ACS Biomater. Sci. Eng.* **2015**, *1*, 260–270. [[CrossRef](#)] [[PubMed](#)]
80. Koepfel, A.; Holland, C. Progress and Trends in Artificial Silk Spinning: A Systematic Review. *ACS Biomater. Sci. Eng.* **2017**, *3*, 226–237. [[CrossRef](#)] [[PubMed](#)]

81. Grínia, M.; Nogueira, R.F.W.; Wellington, C.; Polakiewicz, B.V., Jr.; Andrea, C.D.; Rodas, O.Z.; Higa, M.; Beppu, M. A new method to prepare porous silk fibroin membranes suitable for tissue scaffolding applications. *Appl. Polym. Sci.* **2009**, *114*, 617–623. [[CrossRef](#)]
82. Yang, M.; Shuai, Y.; He, W.; Min, S.; Zhu, L. Preparation of porous scaffolds from silk fibroin extracted from the silk gland of *Bombyx mori* (B. mori). *Int. J. Mol. Sci.* **2012**, *13*, 7762–7775. [[CrossRef](#)] [[PubMed](#)]
83. Cai, Y.; Guo, J.; Chen, C.; Yao, C.; Chung, S.M.; Yao, J.; Lee, I.S.; Kong, X. Silk fibroin membrane used for guided bone tissue regeneration. *Mater. Sci. Eng. C Mater. Biol. Appl.* **2017**, *70*, 148–154. [[CrossRef](#)] [[PubMed](#)]
84. Nuutila, K.; Katayama, S.; Vuola, J.; Kankuri, E. Human Wound-Healing Research: Issues and Perspectives for Studies Using Wide-Scale Analytic Platforms. *Adv. Wound Care* **2014**, *3*, 264–271. [[CrossRef](#)] [[PubMed](#)]